SIGGRAPH ASIA 2011 Tutorial

Thinking in Layers - Modelling with Layered Surfaces

Andrea Weidlich Alexander Wilkie

September 4, 2011

Abstract

This course serves as a guide on the considerable potential of layered surface models that are available in many commercial products.The key advantage of using such layered materials over traditional, more general shading language constructs is that the end result is automatically highly physically plausible because they simulate real materials more precisely. However, this does not mean that these models cannot be used for artistic purposes.

In particular, we demonstrate on simple layered surface models how a surprisingly large number of interesting and important surface types can be efficiently represented. We also show how handy such an approach is for the eventual end user, whose main concern is the ease with which one can describe object appearance based only on a few intuitive parameters.

We first discuss layered surface models in general and the constraints of modelling object appearance in a physically plausible fashion by explaining basic material properties. We then demonstrate the techniques that can be used to analyse such materials, both for high quality offline rendering as well as in a real-time setting before we give examples of the surface types that can be described in this way and demonstrate how we create them in our company.

Course Overview

1 minute: Welcome and Introduction

Andrea Weidlich and Alexander Wilkie

Overview of the course, and motivation for attending it.

24 minutes: Layered Surfaces in Computer Graphics

Alexander Wilkie

This part of the tutorial outlines the main differences to traditional, shader-language based techniques to describe object appearance. State-of-the-art layered surface models in commercial products will be compared. We will also put layered materials in a broader, comparative context with analytic methods or measured BRDFs of more complex materials and discuss when is it appropriate to use them.

25 minutes: Classifying Materials - Using Layered BRDFs to Describe Object Appearance

Alexander Wilkie

In this part of the tutorial we will classify the appearance of different materials into several groups according to their reflectance properties. This is necessary since we later use this groups as a guideline for modelling. This is the technical part of the course since we also discuss physical properties of materials and how they can be transformed into the world of layered materials.

45 minutes: Modelling with Layered Surfaces

Andrea Weidlich

This part of the course showcases the power of layered materials in a practical setting. For some types of surface where BRDF measurements are available, we also discuss the performance of the layered model relative to these measurements, and also compared to other, simpler combined BRDFs. For each type, we discuss the applications, and the limits of the layered approach.

About the Lecturers

Andrea Weidlich

RTT AG Munich, Germany
andrea.weidlich@rtt.ag

Andrea Weidlich is currently a technical artist at RTT AG in Munich in Germany, as well as being an external lecturer at Vienna University of Technology in Austria. Prior to this, she was an assistant professor at Vienna University of Technology, from where she graduated in 2005 with a M.Sc., and from where she received her PhD in 2009. She also graduated with a M.A. in applied media design from the University for Applied Arts Vienna (2011). Her current research interests include predictive rendering with a special focus on appearance modellings.

Alexander Wilkie

Charles University in Prague, Czech Republic
alexander@wilkie.at

Alexander Wilkie is currently a senior lecturer at Charles University in Prague. He achieved his habilitation in Applied Computer Science from Vienna University of Technology in June 2008, and spent the time from 2000 to 2008 as an assistant professor at that university. He obtained both his master's degree (1996) and Ph.D. (2001) in computer science there. His main research interests are predictive rendering, colour science, and appearance modelling. He has authored numerous peer-reviewed papers about computer graphics, and has extensive teaching experience in the areas of photorealistic rendering and colour science, which he obtained both at Vienna University of Technology, and now at Charles University.

Contents

1 Introduction **5**
- 1.1 Motivation . . . 5
- 1.2 Overview of the Course Material . . . 6

2 Layered Surfaces in Computer Graphics **7**
- 2.1 Traditional BRDF Models . . . 7
- 2.2 Reflection Properties . . . 7
- 2.3 Multi-Layer Reflectance Models . . . 9
  - 2.3.1 Layered Models in Academia . . . 9
  - 2.3.2 Layered Models in Production Rendering . . . 9

3 Classifying Materials - Using Layered BRDFs to Describe Object Appearance **12**
- 3.1 Physical Background . . . 12
  - 3.1.1 Light and Spectra . . . 12
  - 3.1.2 Reflection and Refraction . . . 12
  - 3.1.3 Absorption . . . 14
  - 3.1.4 Scattering . . . 14
- 3.2 Composition of Materials . . . 15
  - 3.2.1 Fibers . . . 15
  - 3.2.2 Sparkles and Flakes . . . 16
  - 3.2.3 Intertwining Layers . . . 17
- 3.3 Material Appearance and Visual Clues . . . 17
  - 3.3.1 Metallic vs. Non-Metallic Materials . . . 18
  - 3.3.2 Surface Roughness . . . 18
- 3.4 Classifying Materials According to the Reflection . . . 19

4 Modelling with Layered Surfaces **23**
- 4.1 Parameters . . . 23
- 4.2 Traditional Materials . . . 24
  - 4.2.1 Glossy Paint – Ceramics, Acrylic and Uni Lacquer . . . 24
  - 4.2.2 Frosted Paint – Sugar, Spraypaint and Latex . . . 26
  - 4.2.3 Metallic Foil – Brass and Coloured Metals . . . 26
  - 4.2.4 Metallic Paint – Automotive Lacquer and Metallic Paint . . . 27
  - 4.2.5 Frosted Metal – Metallic Gold and Blue Metallic Paint . . . 27
  - 4.2.6 Patina – Silver Paint and Oxidised Metals . . . 28
  - 4.2.7 Multi-Layer – House Paint and Wood . . . 29

4.3 Special Materials 29
4.3.1 Heterogeneous Surfaces 29
4.3.2 Fluorescent Surfaces 32

A RenderMan Shader **35**

Chapter 1

Introduction

This course material describes the technical and physical details necessary to understand physically plausible layered BRDF models that are available in modern rendering systems. It also highlights numerous practical usage scenarios for such analytical reflectance models.

1.1 Motivation

Modern computer graphics have reached astonishing levels of visual realism and artistic expression. As our technological abilities have progressed, several distinct sub-fields, each with its unique technical challenges and goals, have emerged within the discipline; examples are non-photorealistic rendering, scientific visualisation, production techniques geared for the entertainment industry, or physically based rendering. The latter is a comparatively small but highly interesting area, and is not, as one might surmise from the name, only useful for predictive rendering applications. Techniques from this domain can also be utilised in many contexts for believable rendering purposes, mostly to bring selective realism to scenes that are being assembled under artistic control.

Conventional, believable rendering techniques, such as the workflows used in RenderMan or Maya, have reached a level of capability that is apparently quite sufficient even for highly demanding projects. By contrast, physically based rendering has some way to go before it can be considered equally mature and robustly useful for all application domains that it might be considered for. Significant progress has been made over the past years, but some sub-problems, such as efficient and intuitive appearance modelling under the constraints of such rendering systems, or the still considerable performance penalties associated with unbiased global illumination techniques, are not entirely solved yet.

For the purposes of believable rendering, the normal solution to describing the appearance of an object that cannot be directly modelled using a single BRDF is the use of a shader language. While this approach can deliver good-looking results, it is the time-honored mainstay of most production graphics and not always easily to achieve.

One solution is to resort to using BRDF measurement data for such ”problematic” surfaces instead. While this is of course a viable solution for some applications, this has the drawback of restricting the creativity of the end user: only previously measured surfaces can be applied to objects. Especially for

usage scenarios where physically based techniques are used to augment scenes that are being modelled for artistic purposes, a higher degree of control over object appearance is desirable.

For some of the cases where no simple analytical model exists (such as metallic car paint, or glazed ceramics), layered combinations of several BRDFs could be used instead; this is a fairly obvious approach for all surfaces that have an intrinsic layering. But so far, such true layered surface models have not been in particularly widespread use, mainly because the derivation of a compound BRDF is rather difficult for a truly general arrangement of layers, and exact simulations of light transport in such surfaces are quite costly. However, more and more applications provide layered models, although with varying degree of physical correctness.

The two big advantages of layered models are that they are physically based (if not entirely physically *correct* in the narrow sense of the word because of the approximations that are introduced into the evaluation) and therefore produce feasible looking results, and intuitive to use at comparable low computational costs. However, although we also deal with physically based models, as we will later see this does not limit the usability of such surface models for design purposes. Contrary, we will show that the popular misconception that one can be either physically correct or have freedom in design is not true.

Nevertheless, many artists are trained to shade with single, un-layered surface models; getting accustomed to model in layers means a paradigm shift in the work flow and a new way of thinking. The goal of this course is to comprehensively explain layered surfaces, one of the recent advances in the area of physically plausible appearance modelling. The course briefly reviews the state of the art and the technological challenges in this sub-field of BRDF construction, demonstrates how the simple and efficient approximative combination of layered BRDFs works in practice, and showcases the significant potential of this approach by discussing practical usage scenarios for it.

1.2 Overview of the Course Material

As a means of preparing the ground for the subsequent treatment of the layering, chapter 2 first discusses surface models in general and provides the reader with the physical background that is necessary to truly understand layered materials which will later help in the modelling process. Chapter 3 discusses how materials can be classified to simplify the modelling process, and chapter 4 finally showcases the numerous surface types for which such a layered model can be used, and discusses the potential issues with them. We also compare some of the results with measured BRDFs and go beyond plain, homogenous surfaces and explore the use of such layered BRDFs for the characterisation of the appearance of complex, textured objects.

Chapter 2

Layered Surfaces in Computer Graphics

In this chapter, we briefly review known layered BRDF models and discuss the constraints that physically plausible BRDF models have to fulfil (energy conservation, reciprocity, etc.).

2.1 Traditional BRDF Models

Computer Graphics uses two distinct approaches to deliver realistic surface reflectance behaviour. The first one is the measurement of real surfaces, and the subsequent use of the gathered reflectance data in the rendering process. The second one is the derivation and use of analytical models of varying realism. In this course we focus on the analytical approach.

During the last decades a large number of analytical reflectance models have been developed for computer graphics use. These models can roughly be divided into two groups:

1. *empirical* – and often fundamentally physically implausible – models, which deliver reasonably good-looking results at moderate computational cost, and
2. those where comparatively expensive, *physically plausible* computations of light interacting with matter are used for highly convincing depictions of surfaces.

Especially the more sophisticated specimens of the second category offer a great potential for creating very convincing renderings, but have to be handled with some care. Also, there is only a limited number of BRDF models that are entirely physically plausible, and not all types of common surfaces can be described with them.

2.2 Reflection Properties

In a realistic scene, many different surfaces can be found, and each surface reflects light in a certain way. Many different BRDF models exist that can be used to simulate such reflection. Roughly they can be put into four groups:

- *Specular reflectors* are perfect mirrors, where light bounces off the surface in a mirror like fashion in only one direction,

- *rough specular* surfaces where light is also scattered in directions around the mirror direction, e.g. the Phong model belongs to this category,
- *perfectly diffuse surfaces* that scatter light in every direction over the hemisphere (e.g. Lambertian reflectors) and
- *directional diffuse reflectors* which are a combination of rough specular and perfectly diffuse reflectors, i.e. reflectors that reflect light diffusely, but also have a certain preferred direction. The majority of reflection models belong to the category, e.g. the Cook-Torrance [3] or Ward model [25], and are often formulated with the help of the micro-facet theory.
- arguably, a fifth group of reflectors exists, the group of *retro-reflective reflectors* which are diffuse, but reflect light directionally back in the direction of the incoming light ray, like e.g. the model of Oren and Nayar [21].

An illustration can be seen in figure 2.1. Often traditional BRDF models are only capable of simulating a certain range of reflectance behaviour. For example, Lambertian reflectors can only simulate perfectly diffuse reflection while Fresnel reflectors are perfectly specular reflectors. Models based on a micro-facet approach are used to simulate a bigger range of reflectors. These BRDFs assume the surface to consist of a large number of very small statistically distributed micro-facets, which are oriented according to some given probability distribution function, and which can be either isotropic or anisotropic.

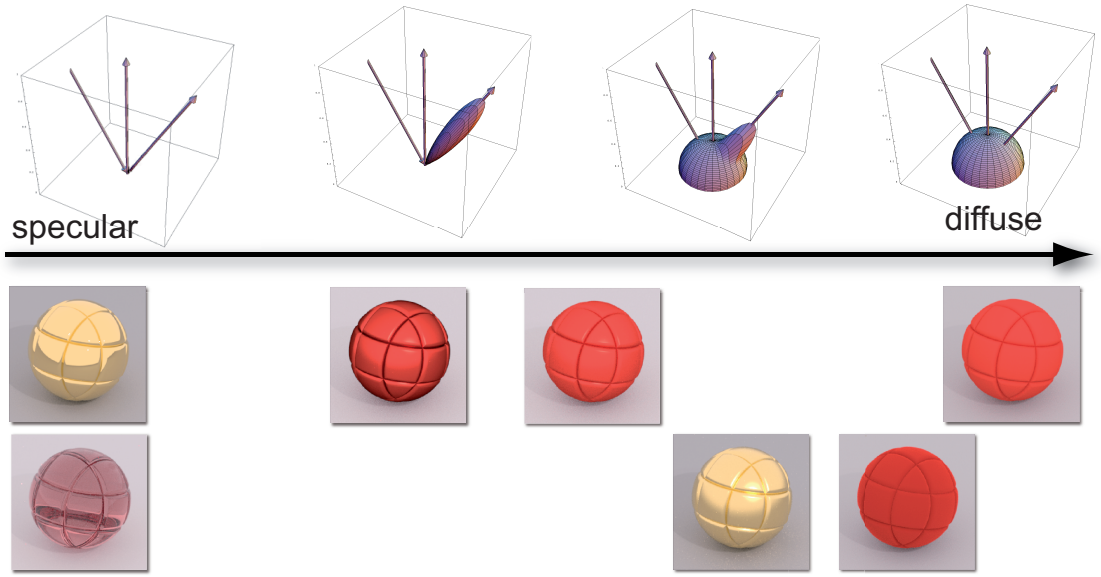

Figure 2.1: Illustration of different reflection types. Top row: Polar plots of perfectly specular, rough specular, directional diffuse and perfectly diffuse BRDFs. Bottom row: spheres rendered with traditional BRDF models that correspond to such a reflection behaviour. From left to right: Fresnel reflector (dielectric and conductor), Phong, Phong and Lambert, Torrance-Sparrow, Oren-Nayar, Lambert.

2.3 Multi-Layer Reflectance Models

Layered surface models offer a great potential for creating very convincing renderings and receive more and more attention in the computer graphics community. Although such models are known in academia for many years, they were hardly used for production rendering until recently. The main difference between research and production models is that the majority of the existing research works aims to solve a specific small topic as e.g. how to render car lacquer with a layered approach, and general solutions are comparable rare. For production rendering, general models like e.g. the MIA shader are of more interest.

2.3.1 Layered Models in Academia

As noted earlier, the idea of using individual surfaces of somewhat limited applicability – such as perfect mirrors or Lambertian surfaces – as layered components of a more sophisticated BRDF, is immediately appealing due to its simplicity and usefulness.

While the concept of using layered surfaces is simple, actually using it in a renderer is not – at least if the unrestricted case is considered, because in this case the computation of the entire BRDF involve sub-surface scattering computations within the layers. A summary of relevant approaches can be found in table 2.1.

Note that although layered surfaces can simulate problematic materials with e.g. interference, sub-surface scattering, dispersion or multilayer finish very well, many surfaces can be reasonable simulated with a simple Cook-Torrance with two microfacet distributions. A good summary can be found in [20].

2.3.2 Layered Models in Production Rendering

Although production rendering was for a long time exclusively in the domain of believable rendering, more and more programs and systems make use of layered models today. However, the level of sophistication varies between the individual systems. While most of them allow only a Photoshop-style layering of the individual components or blending between several models, only a few have a true layering system implemented. In the following we will give a short outlook of material models of three commercial programs with increasing sophistication.

Modo (Luxology)

The Modo material model has a single BRDF as base material with a diffuse and specular term as well as a Dirac reflection and a refraction. Layering is only supported for BRDF parameters, e.g. the diffuse colour or the roughness with different blend modes similar to the modes available in image processing programs, e.g. normal, add, darken.

Materials (i.e. BRDFs) can be stacked, but only with an opacity channel; they do not influence each other. This means that a rough surface on top of a smooth surface will not increase the roughness of the underlying surface (although this would happen in reality). A screenshot of the material interface can be seen in figure 2.2a.

Surface Model	Description	Advantages and Disadvantages
Kubelka and Munk [18], Haase and Meyer [10]	Simulates absorption / scattering of pigments	Highly realistic, limited to piments, no reflection model
Hanrahan and Krueger [11]	Subsurface scattering in layered structures	Expensive, no closed formula, very accurate
Dorsey and Hanrahan [6]	Metallic patinas, based on Kubelka-Munk	Realistic surface aging effects, limited to metallic layers
Neumann and Neumann [19]	One or more perfectly smooth, transparent layer over an arbitrary surface	Includes absorption, physically correct, but no internal reflection, no sampling, no closed formula for entire BRDF, only perfectly specular lacquered objects
Kelemen and Szirmay–Kalos [17]	Cook-Torrance model on top of Lambertian component	Importance sampling possible, special case for smooth and rough lacquer, no absorption, no internal reflection
Wilkie et al. [29]	Diffuse fluorescent surfaces with transparent, rough dielectric layer over a normal diffuse surface	behaviour corresponds to real diffuse fluorescent objects. limited to fluorescent materials
Ershov et al. [8][7], Durikovic et al. [23][24]	Pearlescent paint, statistical model for flakes, Lambertian base with clear coat	Interference, scattering effects, limited to car paint
Icart and Arques [16][15], Hirayama et al. [12] [13] [14]	Multilayered films on conductors, number of layers normally 5 to 6	Includes interference, smooth and rough surfaces
Granier and Heidrich [9]	RGB model	includes interference and dispersion
Dai et al. [4]	transmission through a single smooth or rough thin transparent layer	Light is refracted through thin layer, boundaries can have different roughness, no scattering
Donner et al. [5]	subsurface scattering of skin	Three layers, light can travel between the layers
Weidlich and Wilkie [26]	stacking of arbitrary number of layers, includes absorption and internal reflection	limited to Gaussian distributions, light travels only once between layers, importance sampling possible, general

Table 2.1: Comparison of different layered surface models. Note that this list is by no means complete due to the enormous amount of literature.

Maya (Autodesk)

Maya's LayeredShader allows blending (or mixing) of different materials. However, this is not the same as layering, since the mixing process is reciprocal i.e. if the order the materials is interchanged, the result is still the same. Blending is often used for labeling where an opacity map is used.

Maxwell Render (Next Limit)

The material model of Maxwell allows stacking of different BRDFs, although only one single BRDF model is available. The material model is more physically oriented, parameters can be textured, but they cannot be further manipulated. Two layer blend modes exist, normal and add.

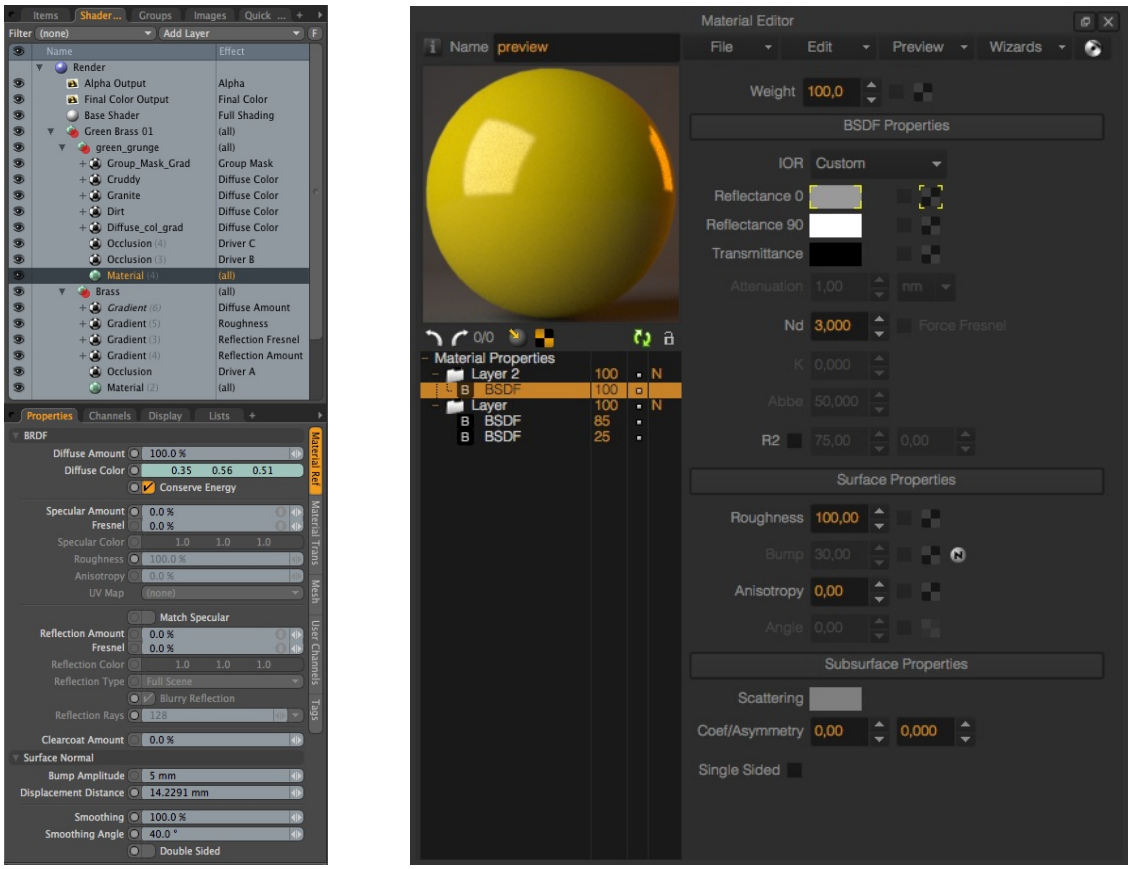

(a) (b)

Figure 2.2: Screenshots of the material interfaces of Modo (left) and Maxwell Render (right). Both systems allow stacking of material components.

Chapter 3

Classifying Materials - Using Layered BRDFs to Describe Object Appearance

In this section we will describe how to use layered surfaces to simulate a variety of different surfaces. We will show that all these different surfaces can be simulated with a simple layered model, with only the layering and the parameters of the individual interfaces and varnish layers being changed. To simplify the modelling process, this section will contain a classification for layered surfaces according to the reflection properties of the individual layers and a physical background that will help the shader artist with the desining process.

3.1 Physical Background

3.1.1 Light and Spectra

When we talk about light, we usually refer to the part that is perceptible to the human eye. This visible part is only a small segment of the electromagnetic spectrum and includes only the wavelengths between 380 and 780 nm. The actual values depend on the observer, but most persons have very similar ranges. Certain wavelengths cause particular visual sensations and are interpreted as colours. For instance, the shortest wavelengths of the visible spectrum can be perceived to be blue or violet and the longest as red. The areas of the spectrum which are adjacent to the visible range are ultraviolet and infrared.

Normally a light ray consists of many different waves with different wavelengths and only appears white if all wavelengths of the visible spectrum are equally represented. The associated distribution of wavelength intensities per wavelength is referred to as the spectrum of a given ray or lightsource. Figure 3.1 shows an example of three different light sources.

3.1.2 Reflection and Refraction

When a light wave strikes an interface between two different media, some of the energy is reflected from that interface, propagates in the mirror direction and stays within the first medium. In most cases,

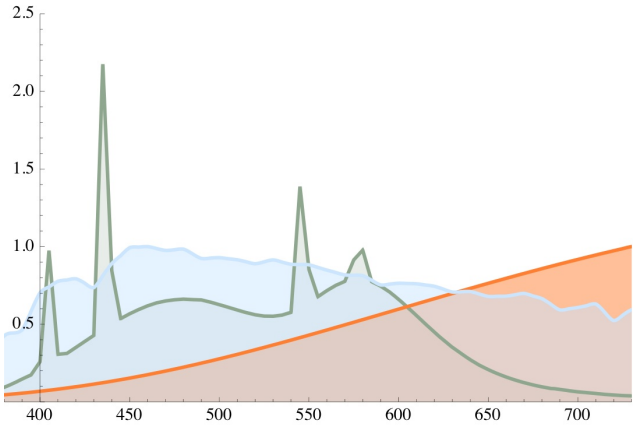

Figure 3.1: Three different light spectra of a light source that resembles candle light (orange), the blue sky (blue) and a flourescent lamp (greenish). Note that the colour of the light depends on the intensity of the individual wavelengths

a part of the incident energy also enters the second medium, and continues its propagation there.

How large this second part is, and in which direction it continues its path, is dependent on the relative density of the two media. Light only propagates in an undisturbed fashion when traveling through a perfect vacuum. In any other medium the atoms that happen to be in the path of a light ray interact with it by absorbing incoming photons, and practically instantaneously reemitting them. The denser a given medium is, and the more frequent these interactions are, the slower light propagates within the medium. As a consequence, if the density of two media is different, the speed of light is changed at the interface between the two, and (except at normal incidence) a change of direction occurs – the light is said to be refracted. The factor by which the velocity of the electromagnetic wave is reduced in proportion to its propagation speed in vacuum c_0 is called index of refraction $n(\lambda)$ and is given by

$$n(\lambda) = \frac{c_0}{v_p(\lambda)} \tag{3.1}$$

where, for a given particular wavelength λ, $v_p(\lambda)$ is the phase velocity of the medium the light wave is entering. The relationship between angle of incidence and angle of refraction of a light wave when traveling between two media with different refractive indices is given by Snell's law

$$n_1(\lambda)\sin\theta_1 = n_2(\lambda)\sin\theta_2 \tag{3.2}$$

where $n_1(\lambda)$ and $n_2(\lambda)$ are the respective, wavelength-dependent refractive indices, and θ_1 and θ_2 are, respectively, the angles between normal and incident, and normal and refracted ray.

Strictly speaking, equation 3.1 is only valid for light that enters a perfectly transparent material. For all materials that do exhibit some form of attenuation when light passes through them, it is convenient to group information about the index of refraction and the attenuation characteristics into a single, complex-valued entity, the complex index of refraction $\tilde{n}(\lambda)$:

$$\tilde{n}(\lambda) = n(\lambda) + i\,k(\lambda), \tag{3.3}$$

where $n(\lambda)$ is the real-valued index of refraction from equation 3.1, and $k(\lambda)$ is referred to as the extinction coefficient (or, sometimes, the absorption index) of the material.

It is worth noting that in principle, all materials can be described by a complex-valued IOR; perfectly transparent materials are simply assumed to have a $k(\lambda)$ of zero. In practice, and in particular in

computer graphics, one usually only encounters $k(\lambda)$ when the Fresnel terms for strongly absorbing media (such as metals) have to be evaluated (as it can be seen in figure 2.2b). But in fact all coloured, transparent objects have an index of refraction with a non-zero imaginary component, even though it is usually quite small for such materials.

3.1.3 Absorption

Usually a part of any refracted light is absorbed inside a transparent material while travelling through it. For most cases, the intensity of this absorption can be described by the Lambert-Beer law. According to it, for a light wave of given wavelength λ, the energy $T(\lambda)$ that is transmitted through a material over a path length of l is related to its initial intensity $I_0(\lambda)$ by

$$T(\lambda) = I_0(\lambda) \cdot e^{-\alpha(\lambda)l} \tag{3.4}$$

The wavelength-dependent constant $\alpha(\lambda)$ is referred to as absorption coefficient, and is a material property that is independent from the path length. The absorbance $A(\lambda)$ of a medium, i.e. the fraction of how much of the entering light is absorbed, is given by

$$A(\lambda) = -\ln T(\lambda) = \alpha(\lambda)l; \tag{3.5}$$

since $A(\lambda)$ is defined as the fraction of incident light that is being absorbed, $I_0(\lambda) = 1$ is assumed.

The Lambert-Beer law can also be written in terms of a logarithm to the base 10, the molar extinction coefficient $\varepsilon(\lambda)$ and concentration c, which is the form commonly used to describe the absorption behaviour of liquid solutions of a given substance

$$T(\lambda) = I_0(\lambda) \cdot 10^{(-\varepsilon(\lambda)cl)}. \tag{3.6}$$

In this particular case, the absorption coefficient $\alpha(\lambda)$ is directly proportional to c and $\varepsilon(\lambda)$ with

$$\alpha(\lambda) = \ln 10 \cdot \varepsilon(\lambda)c \approx 2.303 \cdot \varepsilon(\lambda)c. \tag{3.7}$$

With increasing thinkness or concentration, more and more light is absorbed when traveling through the material. An example of this behaviour can be seen in figure 3.2.

Figure 3.2: Diffuse white spheres with a yellow varnish layer of varying thickness. Layer thickness values are 0.0, 0.2, 0.4, 0.6, 0.8, 1.2, 1.6, 3.0, 5.0, 7.5, 10.0 and 15.0. Note the progressive changes in colour, saturation and hue.

3.1.4 Scattering

How light is scattered by a particle is a function of many things; the particle shape, its size and index of refraction, the wavelength of light as well as the viewing direction. For our purpose, two different types of scattering are of particular interest, *Rayleigh* and *Mie scattering*.

Rayleigh scattering describes scattering from particles that are small compared with the wavelength of light. In particular, Rayleigh scattering can be seen from particles as large as 300nm to particles that are only 1nm in diameter. The intensity of the scattered light is related to the intensity of the incident light by the inverse fourth power of the wavelength λ of the light. This means that the scattering probability for blue light is about 16 times higher than for red light. As a consequence, blue light is scattered much more strongly than red light.

Mie scattering, on the other hand, describes scattering from spherical particles that are larger than the wavelength of light. While in Rayleigh scattering there is a complete symmetry between forward and backward scattering, Mie scattering is much more prominent in the forward direction. Moreover, blue is not the dominant colour. However, with decreasing particle size Mie scattering looks more and more like Rayleigh scattering. Mie scattering is a very prominent feature in milk, clouds or white opals.

Mie scattering calculations soon become very complex, especially if the complex index of refraction has to be considered, which is the case for metallic scatterers. Also, if the scatterers are non-spherical (e.g. rods or hexagons), a different approach has to be used.

3.2 Composition of Materials

Often materials are not homogeneous, i.e. they do not consist of one single material, but have a structure that is not immediately visible from the outside or for the naked eye. This internal structure, however, greatly contributes to the overall appearance of the material.

3.2.1 Fibers

Many materials such as wood, silk but also gemstones consist of fibres. These fibers are either made of a different material and are embeded into the main material like it is the case for example for tiger's eye or Chrysoberyl, or the material entirely consist of fibers (e.g. wood). In both casees, these fibres are arranged in parallel, and when light encounters such a material, a part of the light enters it and when passing through it, the light is scattered on these fibres. Hence the light is not reflected uniformly, but in a certain direction so that it forms a luminous band that moves when the material or the light source is rotated. The sharpness of the band depends on the amount and size of the fibres the smaller and more densely packed the fibres are, the sharper the bright band is. Also, it is noteworthy that the quality of the effect is strongly dependent on the type of the illumination; it is much more prominent under a small light source, like the sun or a penlight. Large-area or multiple light sources diminish the effect.

Macroscopically this effect is visible as anisotropic reflection. For example, the stone in figure 3.3 is a synthetic material that consists of many glass fibres and is cut *en cabochon* so that the fibres are parallel to the base of the stone. This is the best cut since the reflected light is concentrated on a region that is perpendicular to the direction of the inclusions. When the stone is rotated, the luminous bands moves around.

Figure 3.3: Synthetic gemstones that consist of many small, parallel fibres under different illumination. The light is reflected inside the stone, and a luminous band is produced.

3.2.2 Sparkles and Flakes

Another type of inclusions are flakes, small highly reflective metallic particles up to 1 or 2 milimeter in size that are embedded in the parent material. The faces of these tiny particles act as tiny mirrors, so that the material sparkles and glitters when turned around. The effect is found in a number of chemically and crystallographically diverse minerals and stones, such as sunstone, aventurine quartz or goldstone, but also many cosmetic products, paints or metallic lacquer.

One very recognizable type of surface are the metallic paints used by the automotive industry. They consist of metal flakes suspended in a binder, and which are covered by a transparent cover varnish. Optionally, the flakes can be suspended in a tinted binder, or the flakes themselves can be coloured.

Figure 3.4 shows real-life examples of metallic lacquer with flakes. While the colour of the three samples in the left image is constant, it changes towards gazing angles in the right image. The reason for this is that the flakes are coated with very thin layers of a specific substance (often titanium dioxide) which causes interference. Hence certain wavelengths are enhanced while others completely vanish depending on the angle of incidence. Such lacquers are called effect of flip-flop lacquers.

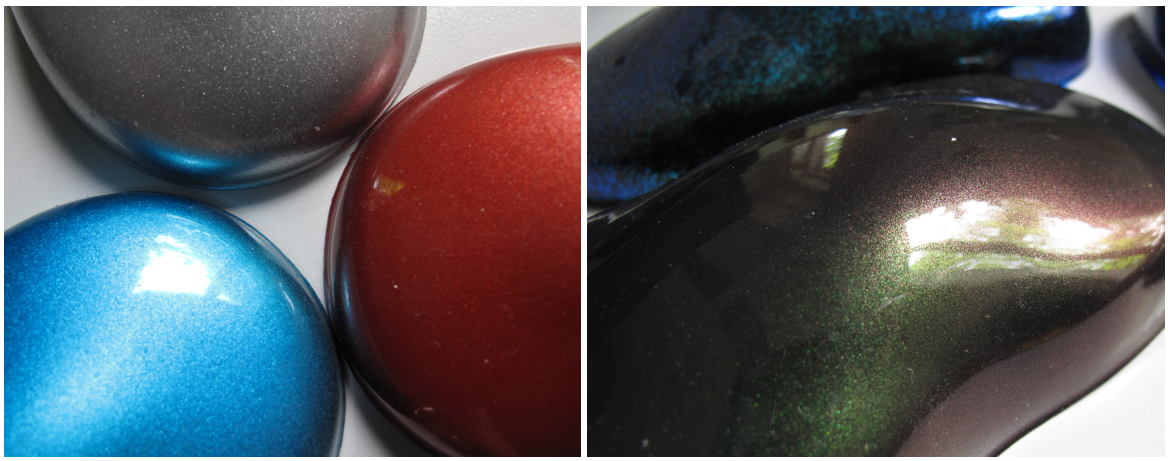

Figure 3.4: Real-life metallic and flip-flop lacquers. Note that the highlights are comparably rough since light is reflected in many different directions.

3.2.3 Intertwining Layers

Sometimes materials are made of two or more different materials that are arranged in thin layers, also called lamellae. Examples of such materials are pearls, beetle shells or certain gemstones. On each of these lamellae, light is partly reflected and partly refracted which, together with the thinness of the layers, can cause significant interference colours.

An example is the *Schiller* effect that can occurs in Labradorite. Such minerals are normally gray, but when they are viewed under certain conditions, vivid metallic colours flash out of the stone. Commonly, these are a very intense bright blue or green, but sometimes also red, gold or violet. The reason for this colour play is that the material is made up from repeated, microscopically thin twinned crystal lamellae. Such twinned structures can appear when two types of crystal with similar structure inter-grow, and both end up sharing the same crystal lattice. The two different crystals form alternating, parallel layers that are approximately 50 to 100 nm thick. On each of these lamellae, light is partly reflected and partly refracted – which, together with the thinness of the layers, can cause significant interference colours. In contrast to most other materials that exhibit this effect, though, the interference colours are highly directional in this case. Figure 3.5 shows a schematic illustration of this effect and a rendered image of this phenomena [28].

As already mentioned, this a similar effect is also responsible for the colour shift of certain metallic lacquers.

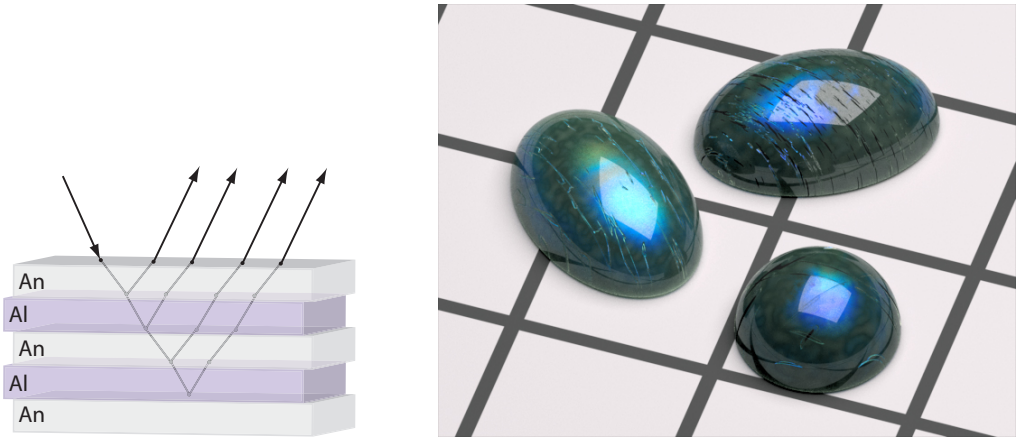

(a) (b)

Figure 3.5: Left: Schematic illustration of reflection and refraction on alternating Albite and Anorithe layers. The reflected light waves can constructively or destructively interfere with each other. Right: Rendered images. The stones are *en carbochon* to maximise the Schiller effect.

3.3 Material Appearance and Visual Clues

Before we can start to model or put materials into certain groups, we first have to answer the question ”What causes the appearance of a material”? Different materials like e.g. sand, velvet or metals have a distinct visual appearance. We are immediately able to distinguish between these materials alone from looking at them, and we immediately know how these materials would feel, if they are e.g. soft, wet or rough. This is possible because the human brain is possible to interpret the features of an object and

concludes from past experiences what we have to expect since it assumes that objects with a similar appearance have similar properties.

These different visual clues are e.g. the blurriness of a highlight which informs us about the surface roughness or its intensity which provides information about the reflectivity of an object. Although the brain does not explicitly try to analyse the physical properties of a material, these clues are strongly related to the surface reflectance properties of an object, which brings us back to our question. Materials look different because they reflect light in a different way and the amount of light that is reflected in a certain direction causes the visual differences between these materials.

3.3.1 Metallic vs. Non-Metallic Materials

The different distribution and intensity of reflected energy is what leads to the different appearance between metallic and non-metallic materials. Event if they are rough, metallic materials reflect the environment much better than non-metallic materials, because metallic materials have a much higher overall reflectivity. When considering the average reflectance over all incident angles, non-metallic surfaces reflect only 4 to 10 percent of the total incoming light. In contrast to that, metallic surfaces reflect, on average, about 80 to 90 percent of the total incoming energy.

Another difference between metallic and non-metallic materials is that for non-metallic materials the reflection intensity is not dependent on the wavelength, i.e. the index of refraction changes only slightly with the wavelength, and no energy is absorbed during reflection. This means that the reflected light has the same colour as the incoming light. However, the situation is quite different for metals; here the index of refraction strongly depends on the wavelength and often certain wavelengths are absorbed; consequently metallic materials change the colour of the incoming light.

Figure 3.6 illustrates this concept. Figure 3.6a shows three metallic spheres, made of gold, silver and copper. The highlights of the gold and copper spheres are coloured, because the gold sphere absorbs the blue part of the light, while the copper sphere reflects only reddish light and absorbs the rest. Note that this is not the case for the silver sphere, since silver, and white metals in general, reflect all light more or less equally, independent of its wavelength.

Figure 3.6b and 3.6c further demonstrate the difference between metallic and non-metallic materials. To match the appearance, the metallic spheres in figure 3.6b have been coated with a coloured lacquer so that they have the same colour as the non-metallic spheres in 3.6c, and the respective spheres have the same degree of roughness. Still, both images look quite different; although the non-metallic spheres do reflect the environment, the reflection is only weak, and the colours of the spheres are much more prominent. In contrast to that, reflections of the other objects can be clearly seen in the metallic spheres, especially in the purple sphere.

3.3.2 Surface Roughness

The surface highlight is the most important visual clue to estimate the surface roughness. One of the fundamental physical principles, the law of reflection, is that light is always reflected in the mirror direction, i.e. that the incoming angle equals the outgoing angle. This is, however, on a macroscopic level only true for very smooth materials. With increasing surface roughness from e.g. scratches or

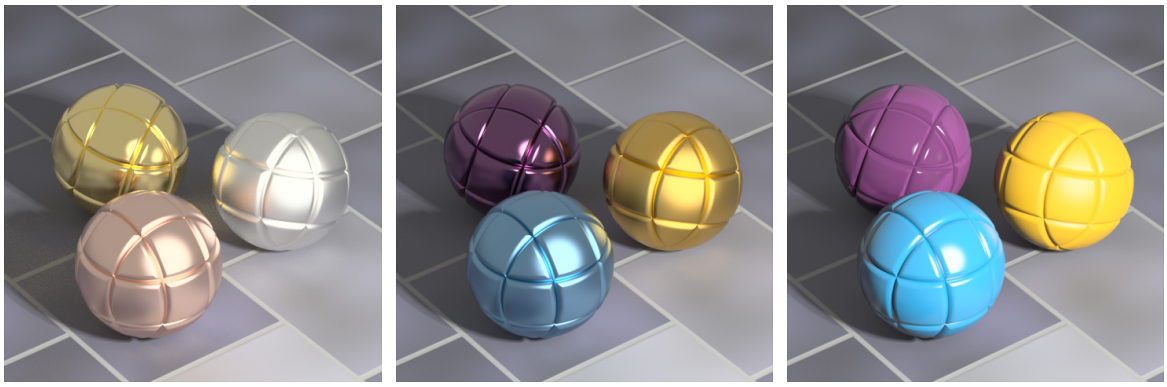

(a) (b) (c)

Figure 3.6: Metallic, coated metallic and non-metallic spheres. The respective spheres in 3.6b and 3.6c have the same colour and roughness, but still look different.

imperfections, light is also reflected not only in the ideal direction, but also offset from the ideal specular angle due to microscopic surface variations. This results in a broader, but less intense highlight, since the incoming energy is reflected in many different directions. The reflection becomes more and more diffuse until the same amount of energy is reflected in every direction over the hemisphere.

As it can be seen in figure 3.7, both metallic and non-metallic surfaces exist in various degrees of surface roughness. However, with increasing roughness the highlight is not focused anymore and starts to vanish.

3.4 Classifying Materials According to the Reflection

To simplify the modeling process, we will now propose a decision tree that allows us to put materials into groups. For our purpose, we will classify materials according to their reflectance behaviour instead of using every day language like e.g. gloss or luster. The full decision tree can be seen in figure 3.8.

The first decision we have to make is if we want to simulate a metallic or a non-metallic surface. If the environment is visible, i.e. the object is highly reflective, or if the highlight is coloured, the material we want to simulate is, with a very high probability, metallic.

For non-metallic materials, the next decision is pretty easy. If the material we want to simulate has a clear reflection of the lightsource, i.e. the highlight is sharp, it falls into the group of ”smooth surfaces on top of a diffuse surface”, it is a surface that specularly reflects light from the top, while the remaining part of the energy enters the material, is partly absorbed there and re-emerges in a diffuse way. We call this group ”glossy paint” after its most obvious representative. Materials that exhibit such a behaviour are e.g. smooth plastics, smooth ceramics of lacquer. Otherwise, if the lightsource is blurred or not even visible, the material falls into the ”frosted paint” group – a rough layer over diffuse surfaces. Such a materials are e.g. rough plastic, rubber, paper or wall paint.

Metals are a little bit more complicated to classify. Metallic surfaces that clearly reflect the environment belong to the group of ”smooth layer on top of a smooth surface” which is called ”metallic foils”; they are smooth metallic materials that are coated with a smooth transparent varnish layer. Classical

Figure 3.7: Several non-metallic (top) and metallic (bottom) real world materials with different degree of roughness. Note the broadening and vanishing of the highlight.

examples are e.g. christmas ornaments that are made of glass and coated on their interior with a silver nitrate solution.

On the other side, if the environment is somewhat visible, but blurred, at least one rough component is involved. Surfaces that still have a sharp highlight, or a clearly visible, but weak reflection of the environment, are put into the group of ”smooth layer on top of a rough surface” which we call ”metallic paint”. They consist of a rough metallic base material that is coated with a smooth varnish. A typical representative that falls into this group is metallic car paint, but also, as we will later see in section 4.3.1, all sorts of metallic inclusions belong to this group.

Finally, materials that are metallic but have only a weak and blurry highlight – or none at all – must have a rough top surface. The only question is now if this rough top surface coats a smooth or a rough metallic base material. The only indicator we have for this is the width of the highlight. Surfaces that fall into the group of ”rough layer on top of a smooth surface”, called the ”frosted metal”-group, tend to have a smaller highlight than the materials that belong to the ”patina”-group, the group of ”rough layer on top of a rough surface”. Also, completely rough surfaces should have a smaller and a broader highlight.

The final classification can be seen in figure 3.9, although it should be noted that this is probably not an exhaustive list of what can be achieved by this technique. Note that there are 8 instead of 6 types. One represents the further split into tinted and non-tinted varnish that can be performed for all types, and one stands for the group of materials that consists of more than two layers, i.e. multi-layered materials.

Another starting point could be the reverse direction, namely to use these categories in the context of a material library where several possibilities are provided and the user can pick a materials that

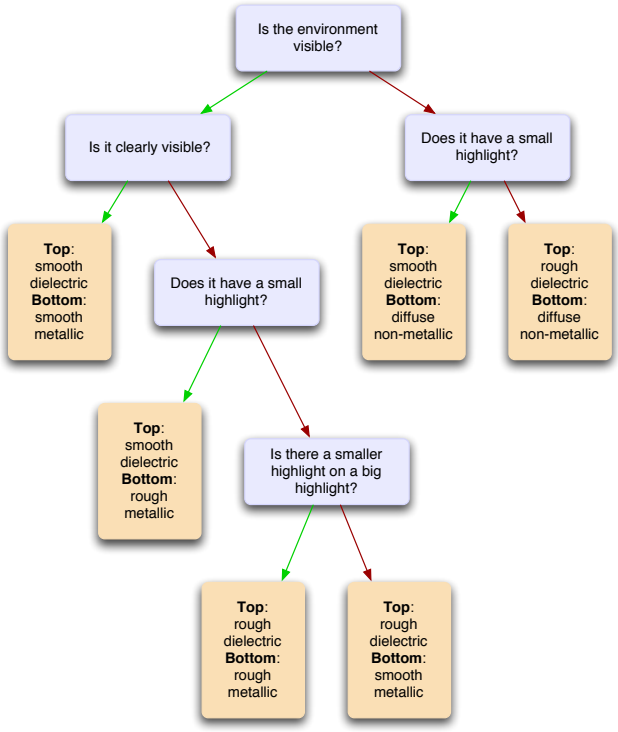

Figure 3.8: Illustration of the decision tree. Green arrows indicate positive decisions, red negative. We can build six basic groups of materials on the basis of their reflection properties.

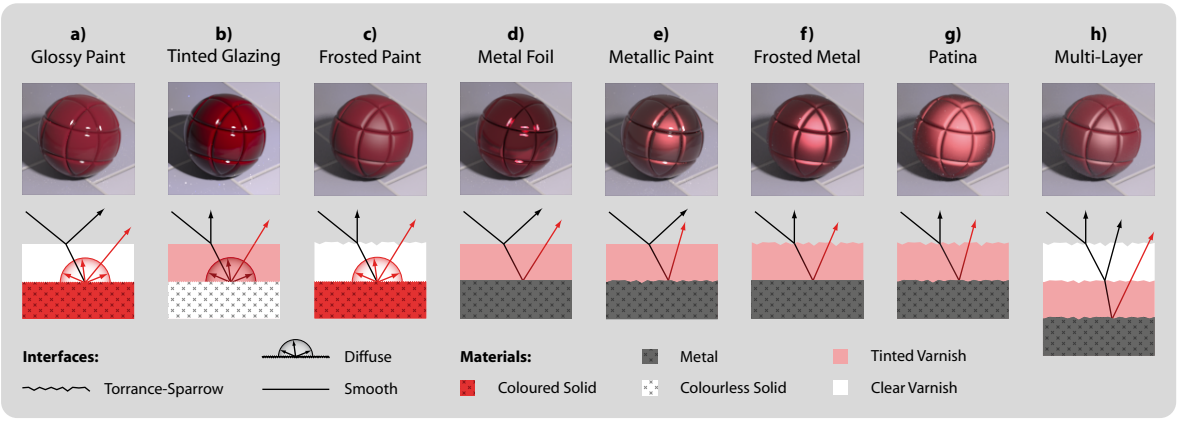

Figure 3.9: Examples of various surface types that can be generated by using our layered model in different configurations. In order to properly distinguish the various cases the icons do not exhibit the simplifying assumption shown in figure **??** which we use for all our actual BRDF computations. The micro-facets are much smaller than the layer thickness in this drawing.

has similar appearance attributes. By slightly changing the parameters the user can now adjust the material. Additionally it is possible to create completely new materials by using random numbers for the parameters or by interpolating between several existing ones; the first one is technically possible due to the small set of input parameters and the latter one because all different materials use exactly the same set of parameters (since they use the same shader).

Chapter 4

Modelling with Layered Surfaces

After discussing the general capabilities of layered surfaces, and after presenting a methodology for using such materials, we give practical examples of how certain materials can be modelled by this approach. To simulate these materials, we used the Renderman shader code that can be found in the appendix and is an implementation of the surface model of [26]. The fact that the same BRDF layering code is used for all of them underlines that a large variety of different surfaces can be simulated using a single module, with only the layering and the parameters of the individual interfaces and varnish layers being changed. In the interest of reducing the complexity of this demonstration section, we only used the original Torrance-Sparrow model [22] and the Oren-Nayar model [21] as basic components f_{r_n} for these layered BRDFs. All examples except figure 4.2c and 4.4 were inspired by BRDF measurements from Cornell [1] and MERL [2].

4.1 Parameters

One big advantage of the presented approach is that a variety of different surfaces can be produced with comparably few parameters. While it is possible to include more effects like e.g. bump mapping which would increase the number of parameters, the following examples used the basic parameters introduced before:

- **Top surface roughness.** The roughness of the varnish is given in degrees and influences the size of the highlight.
- **Index of refraction top surface.** The IOR is given as float value and specifies the intensity of the reflectivity/intensity of the highlight. Note that in this context it is possible to replace the IOR with a more intuitive term that e.g. ranges between 0 for not reflection and 1 for very reflective[1] (or a more sophisticated formula that allows more freedom in the design process) as

[1] A very simple possible formula for a parameter that varies between 0 and 1 would be for example the following:

$$IOR = 1 + (parameter * parameter) * 5.0 \tag{4.1}$$

The formula non-lineally converts an empirical reflection parameter into an refractive index that lies between 1 and 5; as it can be seen in table 4.1, real-life coatings normally have values between 1.3 and 1.8, albeit for a more metallic appearance a higher reflectivity is sometimes desired.

it is commonly done among artists; as long as this parameter is internally converted to an IOR there are no limitations.

- **Layer thickness.** The thickness of the layer influences hue/value of the varnish.
- **Absorption properties of the layer.** This is actually only a RGB colour and adds additional colour to the base layer.
- **Bottom surface roughness.** This is the counterpart of the first parameter. Since we use the Oren-Nayar model non-metallic materials, and the sigma is in fact a further increase in surface roughness, these two properties can be combined in one parameter.
- **Index of refraction/colour bottom surface.** For metals, the IOR is not a simple float, but two sets of RGB values since metals have a wavelength-dependent complex IOR. We can also use one of the RGB values to store the colour of a non-metallic material. Note that again we can replace the IOR with e.g. a reflection parameter and a colour.

Which leads us to a set of six variables[2]. The advantage of such a small set of variables is that the design process becomes more and more complex with an increasing number of variables. Commercially available shaders have often a set of 30 to 40 variables which are hard to handle for non-experts. An exemplary interface can be seen in figure 4.1.

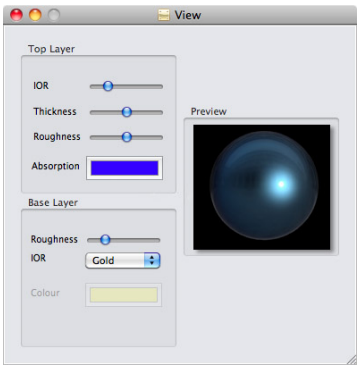

Figure 4.1: A simple GUI is sufficient to simulate all kind of different materials with just a few sliders. Note that for the base layer either the IOR or the colour is active. Which one depends on the roughness of the base slider.

4.2 Traditional Materials

4.2.1 Glossy Paint – Ceramics, Acrylic and Uni Lacquer

A typical application for a diffuse surface covered with a smooth layer is the simulation of glossy paint, opaque ceramic glazing, as well as plastics; examples can be seen in figure 4.11.

To model these materials, a perfectly diffuse surface is used as base material. To limit the number of different BRDF components used in this section, we decided to use an Oren-Nayar surface with roughness of 0.0° instead of the more obvious Lambert surface; this caused a slight performance hit. If performance were a critical consideration, one would of course use a Lambert surface instead.

[2]If we deal with more than two layers, parameters 1 to 5 have to be repeated and the numbers of parameters is increased.

The advantage of using an Oren-Nayar surface is that we could also simulate backscattering, which, however, is comparable rare for glossy objects.

The upper layer is a smooth Torrance Sparrow layer; the roughness is normally a value between 0.01° for very smooth, almost perfect surfaces and 3° or 4° for surfaces that are smooth, but have little imperfections like e.g. very small scratches which gives them a slightly rough appearance. The difference can be seen in figure 4.2. For the green green acrylic lacquer in figure 4.2a, a surface roughness of 3.5° was used; consequently the highlight is a little bit blurry. The blue sphere looks much smoother than the red one although the index of refraction is 1.7 for both spheres and both have a perfectly diffuse base. The differnece between both is that for the blue sphere we used a roughness of 0.01° while the red one has a roughness of 1.5°.

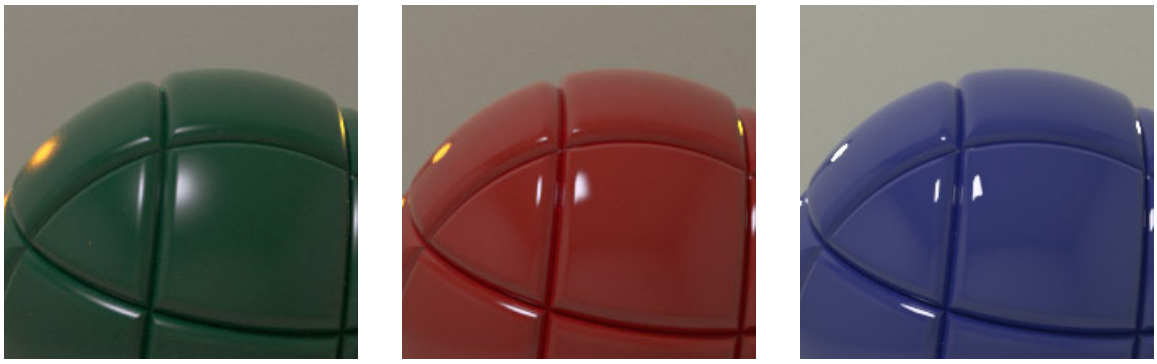

(a) (b) (c)

Figure 4.2: Magnification of figure 4.2a, 4.2b and 4.2c with decreasing roughness. For the green sphere, a lower IOR (1.5) was used than for the red and the blue sphere.

The clear varnish of such objects has normally an index of refraction between 1.35 and 1.7. Typical transparent varnishes are

Varnish	IOR
Ice	1.31
Teflon	1.35
Acrylic laquer	1.45
Glass (quartz)	1.46
Plastics	1.53
Ceramic glazing	1.7

Table 4.1: Index of refraction for several typical varnish materials.

Choosing a higher index of refraction is often unrealistic for dielectric materials.

In addition, the lacquer layer can be tinted as it is the case for the sphere in figure 4.11k. For completely transparent lacquer layers, the thickness of the layer can be neglected (as it is the case for the blue and the green sphere) since no absorption occurs, but for tinted varnishes, the layer thickness respectively the degree of absorption plays an important role. In surfaces of this type, the colour usually increases in saturation towards grazing angles, where the colour of the sphere in figure 4.11o largely stays the same everywhere on the object regardless of curvature. However, since the varnish layer has to be comparatively thin, is has to be strongly absorbing.

4.2.2 Frosted Paint – Sugar, Spraypaint and Latex

Frosted paint materials generally have a low gloss component (see table 4.1), but in contrast to the *glossy paint* materials, the surface roughness is between 5° and 40°. This leads to a less intense, but broader highlight. Examples can be seen in 4.11a, 4.11h and 4.11l.

Figure 4.11a shows a red garnet sphere that has been coated with a gloss-reducing finish; this is one of the examples from the Cornell BRDF database [1]. We combined a red Oren-Nayar base with no surface roughness (i.e. a Lambertian surface) with a varnish of moderate roughness. The average micro-facet slope is 10° and the refractive index of the varnish is 1.5. Here, the varnish layer is clear and can be neglected as it is the case for the other two examples.

The sugar sphere in figure 4.11h is covered by a layered surface that consists of a neutrally coloured Oren-Nayar base with a sigma of 0.26, covered by a very rough ($m = 26°$) and completely transparent rough layer. The IOR is that of real sugar (which is at about 1.35). This combination leads to a surface with very weak highlights, like a real sphere made of compacted sugar would exhibit.

The green latex sphere in figure 4.11l uses similar values, except that this kind of surface is even more back scattering, therefore the Oren-Nayar sigma is now 0.34, and that the Oren-Nayar surface is coloured green. The IOR of the transparent, rough top layer is even lower than on the sugar sphere ($n = 1.3$). This might be a little bit unrealistic (although latex exist that has such a low IOR, real latex normally has an IOR of 1.5), but a comparison with measured data showed that this value works best.

4.2.3 Metallic Foil – Brass and Coloured Metals

A very typical appearance results if a smooth, colourless metal is covered by a smooth, tinted layer of varnish. The iconic object for such surfaces are christmas orbs, but polished brass surfaces such as figure 4.11g also belong to this category. The roughness of the smooth dielectric varnish lies again between 0.01° for very smooth and 3° or 4° for surfaces with small imperfections. Care should be taken that the roughness of the top surface increases the roughness of the next surface. Therefore the *sum* of top and base roughness of the metallic surface should not be larger than 4°.

Another difference is that for metallic surfaces, a single index of refraction is not sufficient since the index of refraction for metallic surfaces is complex and wavelength dependent. Therefore it has to be computed for each RGB component. Typical values are

Metal	n	k
Gold	(0.1,0.42,1.56)	(3.8, 2.5, 1.9)
Silver	(0.14,0.13,0.157)	(4.44, 3.25, 2.40)
Aluminium	(1.94, 1.0, 0.6)	(8.21,6.69,4.86)

Table 4.2: Real and imaginary index of refraction for gold, silver and aluminium.

Values for other metals can be found in standard physics textbooks (B=450nm, G=525nm and R=680nm).

The brass material is a good example that the layering approach can also be used to successfully jerry-rig appearances, instead of always using it to exactly simulate the behaviour of real materials. Certain materials have frayed highlights that can not be simulated with a single, unlayered Torrence-Sparrow

surface. To simulate this effect, two transparent layers were stacked, the first one has an IOR of 1.0 (which means that no reflection occurs and all the light enters the material), but is tinted. The next layer is an almost perfectly smooth ($m = 1°$), tinted varnish layer with an IOR of 2.0. Without the first (invisible) varnish, the second varnish would have a white highlight, which is not the case for metallic materials. The base layer is a slightly rough ($m = 3°$) golden material. This gives a very good approximation of the desired appearance.

4.2.4 Metallic Paint – Automotive Lacquer and Metallic Paint

One very recognizable type of surface are the metallic paints used by the automotive industry. They consist of metal flakes suspended a binder, and which are covered by a transparent cover varnish. Optionally, the flakes can be suspended in a tinted binder, or the flakes themselves can be coloured.

Such materials always have a surface roughness of at least $m = 5°$. It turned out that a roughness of $12°$ to $14°$ is a good value to simulate the directional diffuse reflection of metallic car lacquer, but higher values are also possible.

For example, to model the material used for the sphere in figure 4.11b one uses a rough ($m = 12°$), neutrally coloured metallic basis, and covers this with a strongly tinted, smooth ($m = 1°$) layer of varnish. In this context it is not desirable to have a perfectly smooth top surface (e.g. $m = 0.01°$), since real car lacquer is never perfectly smooth.

Since this is a fairly good approximation of real metallic paint in terms of structure, it is not surprising that the sphere in figure 4.11b shows all the expected effects, such as darkening towards the edges, and a deep colouring that reveals metallic characteristics only for steep viewing angles. Unsurprisingly, the parameters for the paint shown in figure 4.11b correspond fairly closely to what one would expect to find in a real metallic paint.

For the second sample, the gold metallic paint shown in figure 4.11d, this is quite as true. For the top layer, the IOR needed for a close correspondence with the measurements is 1.85, which is too high for normal varnish (normally an IOR of 1.5 is used, as it was the case for figure 4.11b), but gives a silverly, slightly pearlescent appearance. However, such a high IOR could be seen as simulating a varnish layer with increased reflectivity, e.g. a layer with additional, small metal flakes in it. Again, the varnish is tinted.

If one relinquishes the simulation of individual flakes (which, at least for settings that do not involve extremely close-up viewing, is usually permissible), this sort of paint lends itself to a layered modelling approach exceedingly well (see section 4.3.1).

Note that if one wants to simulate fip-flop lacquer, the view-dependent colour has to be taken into account. A possible – albeit not physically correct – solution would be to create two different rough layers with different colour and invert the Fresnel effect for one of the layers.

4.2.5 Frosted Metal – Metallic Gold and Blue Metallic Paint

A surprisingly big number of materials can be simulated by stacking a rough material on top of a smooth metallic material. Again, the top surface has a surface roughness of at least $5°$, but for most surfaces the surface roughness lies between $10°$ and $20°$. In contrast to that, the metallic base surface

is smooth, but, as already pointed out, the rough top surface ”turns” the base surface into a rough one, so the effective roughness of both surfaces is more or less the same. Consequently the highlight of both surfaces is approximately the same.

This can be seen e.g. in figure4.11j. The real material, gold paint, has a smooth metal shine, with fine aluminum powder and pigments to obtain the shine with tiny bright spots that are caused by mirror like flakes which are visible on grazing angles. As base surface a smooth (m=1°) golden material was used, the varnish is slightly tinted to simulate the reddish colour. The top layer is rough (m=13°) – so the effective roughness of the base layer is m=14° – and has a weak index of refraction of 1.3 to suppress strong reflections at grazing angles. Note that if we would use a simple rough golden metallic surface (e.g. the traditional Torrance-Sparrow surface), the result would be quite different, because coated materials reflect light at grazing angles in a different way.

Figure 4.11i, blue metallic paint, is another surface of that type: a fairly smooth aluminum base ($m = 1°$) covered by a rough ($m = 17°$), tinted dielectric layer. The IOR is slightly higher (1.5) and the varnish clearly tinted to produce the blue colour.

4.2.6 Patina – Silver Paint and Oxidised Metals

Rough-over-rough material are arguably the rarest of the surface types discussed here. The silver paint in figure 4.11eis such a surface: a silver base ($m = 10°$) covered by a colourless ($m = 7°$) dielectric layer of moderate IOR 1.7. Such surfaces are – depending on the actual roughness values – can be considered as diffuse surfaces.

The visual difference between surfaces that fall into the rough/rough category and surfaces that belong to the rough/smooth category is rather subtile; the most prominent visual difference is that the fall-off of the highlight is different. *Frosted metal* surfaces have only a single highlight with linear fall-off while *Patina* materials actually have two highlights, a sharper one on top of a broader one; this leads to a non-linear fall-off. The difference can be seen in figure 4.3.

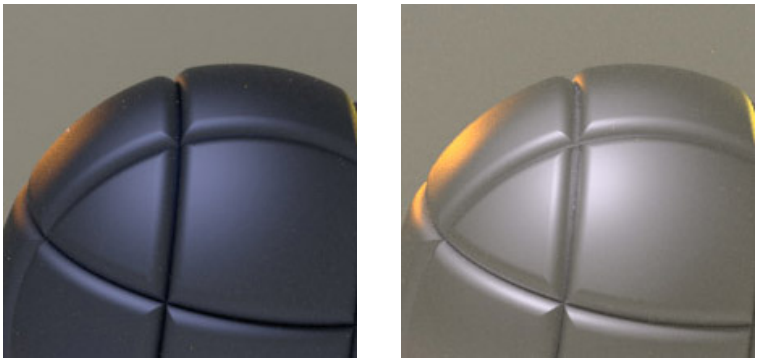

(a) (b)

Figure 4.3: Magnification of figure 4.11i and 4.11e. Both surfaces have the same effective roughness of $m = 17°$, but the form of the highlight is different.

4.2.7 Multi-Layer – House Paint and Wood

Some examples of the Cornell and MERL BRDF measurement databases do not lend themselves easily to simulation by a single layer set-up. In some cases, such as the light blue house paint, two layers atop a base substrate are needed to match the behaviour of the targeted material. In particular, matching the highlight shapes of a given object can require additional layers if the material in question exhibits features such as a strong fan-out of highlights.

In the case of the light blue house paint example shown in figure 4.11c, two transparent layers of equal IOR 1.3 are stacked atop a bluish coloured Oren-Nayar base with sigma 0.34. The top layer has $m = 30°$, while the lower has $m = 7°$. The combination of the rough top layer over the intermediate, not so rough transparent layer creates the highlight shape one sees in the result.

Another material that can be simulated with several material layers are decorative wood. As already mentioned, wood has a very distinct appearance due to its fibre structure. Often, wood is modeled with an anisotropic surface model like e.g. the Ward or the Ashikhmin-Shirley model. However, these models are not capable of capturing the phenomenon that – if tilted – a shine will appear that wanders along the structure.

A better approach is to use a base diffuse Lambertian layer with a texture that simulates the diffuse scattering, i.e. the wood colour. On top, a rough layer is put which is also textured, but has a normal map that tilts all normals to the left or rights. The purpose of this layer is to simulate the behaviour that light is not reflected on the material interface itself, but enters the structure and is reflected on the fiber structure that is tilted in a certain direction. Additionally, another low gloss component is used to capture the light that is reflected on the interface. Figure 4.4 shows an example of a material that was created like this.

Figure 4.4: Interior of a Porsche Panamera. rendered with DeltaGen. The wood was rendered with the approach described in section 4.2.7.

4.3 Special Materials

4.3.1 Heterogeneous Surfaces

Many natural materials are coloured more or less irregularly, an effect that cannot be adequately described by a single layered surface model alone. In this section, we present two examples of how one can efficiently model more complex structures by combining layered surfaces with procedural textures [27]. In this context we use layered surfaces with different parameters, and use them as texture input to produce heterogeneous structures.

(a) (b)

Figure 4.5: **(a)** Samples of various almost opaque, aventurescent minerals, Lavender Lepidolite (left stone), Raspberry Aventurine (top right) and a Green Aventurine specimen (middle). **(b)** Example renderings of various forms of Sunstone. The metallic glitter and orientation-dependent sheen have made this particular mineral a sought after gemstone. Note that only the specimen on the top right is opaque; the other two are translucent, volumetric objects with a glitter map.

As case study we describe the modeling of aventurescence in gemstones (see figure 4.5), a glittering effect that is caused by small, crystalline metallic inclusions in a parent mineral with a highly reflective surface of up to 1mm in size, but similar approach can be used to e.g. model flakes in a metallic lacquer. The obvious benefit of using layered surfaces in this context is that even though the shader-based texture patterns that govern the appearance of these objects are more or less ad-hoc creations, the overall appearance of these stones is still highly physically plausible, since the individual texture components are realistic.

As discussed in detail in [27], the core of achieving results such as those shown in figure 4.5 is the use of procedural texture layers, each of which contains surfaces that are described by layered BRDFs. Figure 4.6 shows an overview of how various layered BRDFs can be integrated into a system of specialised Voronoi textures. In the following two sections, we briefly discuss the details of two of the gemstones shown in figure 4.5, namely the Lavender Lepidolite and the Sunstone specimens.

The overall modelling of the Lavender Lepidolite in figure 4.5 can be inferred from figures 4.6 (for the basic idea behind the pattern) and 4.7 (for the variations in the pattern). The surface map of the dark tiles has 9 entries, but in contrast to the Aventurine glass, most of the surfaces have a Lambertian base of different colour (we used 6 different colours) and a smooth layer with index of refraction of 1.56. Only one entry has a metallic (in this case a silver) base with an average micro-facet slope of 1 degree. The layer is smooth and pinkish (similar to the colour of the tiles). The second surface map of the bright tiles is build similar, except that the colour of the Lambertian bases are brighter. Here we used only 5 different colours. Dark and bright tiles have the same size and are put in another surface map with bigger tiles.

The third surface map for the marble inclusions has only 3 surface entries which are even brighter than the bright tiles, but to disrupt the otherwise continuous line, entries from the bright and from the dark tiles are also used. Please note that the tiles of the marble surface map are much smaller than the dark or bright tiles.

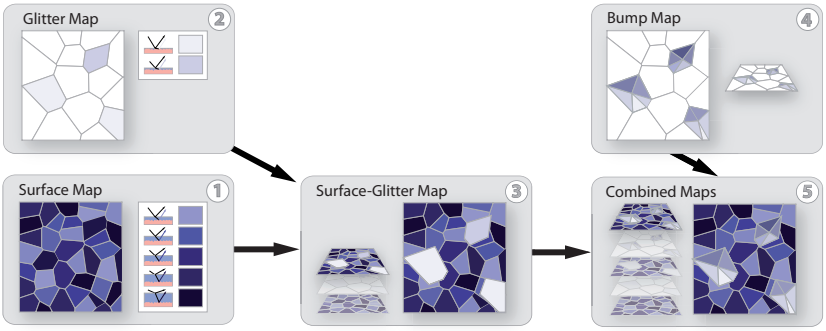

Figure 4.6: Schematic illustration of the spatial arrangement of the Voronoi cell texture layers. The cells of textures that represent individual particle facets located on a deeper level are smaller (component ① - the Surface Map) , and the texture layer nearer to the top (layer ② - the Glitter Map) includes fewer and larger cells that are assumed to stand for entire particles. Most of the cells in ② are completely transparent, with only those responsible for the glitter remaining. Component ④ - the crystal facet bump map - provides sparkle facets for exactly those cells in layer ② that are not transparent. *Note that the varying colour of the bump map facets in this drawing is **not** due to different types of surface being used, but due to shading effects of the now non-planar surface!* The combined result ⑤ mostly consists of polygonal facets of varying colour intensity, with some of them exhibiting additional sparkling effects due to their modified surface normal.

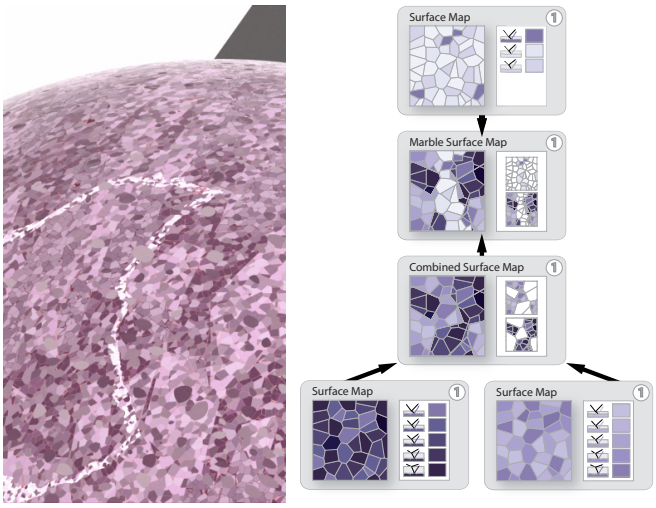

(a) (b)

Figure 4.7: **(a)** A close-up of the Lepidolite from figure 4.5, which reveals that – like in a real stone of this type – the overall appearance of the stone is caused by a complex pattern of polygonal particle facets, which are further influenced by colour changes driven by low-frequency, marble-like patterns within the material. To produce this effect, the simple arrangement of layered surfaces used for Aventurine Glass in [27] is replaced by a more complex combination of various surface maps outlined in **(b)**. Each of these maps in turn consists of several layered surface elements, and a procedural marble texture function is used to switch between the individual maps.

The glitter map is built similar to that of the Aventurine glass with 4 entries. They have a silver base, but otherwise everything is the same. Only very few entries of the glitter map are filled.

Unlike the Lavender Lepidolite, the opaque Sunstone on the top right of figure 4.5 has no surface map, because it is so opaque that hardly any variation in colour can be seen. Therefore we used the same Torrance-Sparrow surface with a Lambertian base and smooth varnish to fill all transparent tiles of the glitter map. Note that we used the reflection spectrum of a real Sunstone for the colour.

The glitter map has again four entries. The base material of the glitter is copper, the average micro-facet slope is 3 degrees. The varnish has the colour of the Lambertian base and has an index of refraction of 1.58. The average micro-facet slope is 4 degrees. The relation between glitter and non-glitter tiles is as is the case of Aventurine glass. The glitter map has 3 entries, the base material is copper and the average micro-facet slope is 5 degrees. The tiles are tinted with the same colour the stone exhibits. The pink stone exhibits much more glitter, because many cells of the glitter map are filled. In contrast to that, the patterned Sunstone has less glitter, but the scattering function is no longer homogeneous. To produce the desired effect we combined three different Perlin functions with different parameters. The index of refraction is again 1.58 for both stones.

4.3.2 Fluorescent Surfaces

A less obvious application of layered surfaces is to use them to simulate reflection from fluorescent surfaces [29]. Unlike normal surfaces that just reflect more or less incident light depending on the viewing and illumination geometry, fluorescent surfaces have the unusual property that they can also change the wavelength of the reflected light through processes at the molecular level of the surface pigments. A remarkable property of fluorescent surfaces is that the reflection colour is directionally dependent. This effect can be seen in figure 4.9, where a green laser beam with different angle of incidence is reflected from an orange fluorescent day-glo cardboard sample, and can be easily replicated by anyone with access to a green laser pointer and a piece of day-glo cardboard. Note that while the bright dot where the laser hits the surface – and also parts of the reflection pattern – are a bright orange caused by the frequency shift typical for this kind of fluorescent colorant, other parts of the reflection – essentially the specular component – are still the native green of the incident laser beam.

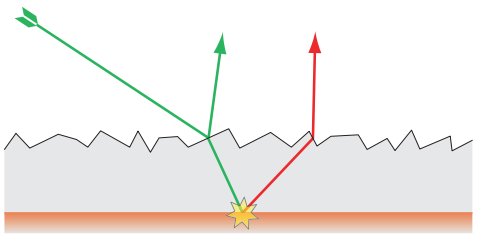

Figure 4.8: Concept of the rough varnish microfacet model used for the diffuse fluorescent BRDF needed to model the surface behaviour seen in figure 4.9. A rough layer of transparent Fresnel facets is assumed to cover a thin layer of transparent varnish on top of a fluorescent Lambertian base layer. Fluorescence only takes place for those rays that come in contact with the base layer.

As discussed in [29], this sort of bi-coloured reflection behaviour is pretty much intractable with normal, single-model BRDFs and normal combinations of BRDFs (such as the classical "Phong plus Lambert" model). However, a rough varnish type layering (the logic behind which can be seen in

figure 4.8) can capture this sort of reflectance pattern quite well, and with minimal modelling effort. It is important to note that this usefulness of layered models for fluorescent BRDFs does not stop here: specular fluorescent paint, such as the paint found on ambulances and police cars (which also exhibits the bi-colored patterns, only in a much more focused way), is of course also easily modelled as a ”glossy paint” surface, with the diffuse undercoat being fluorescent.

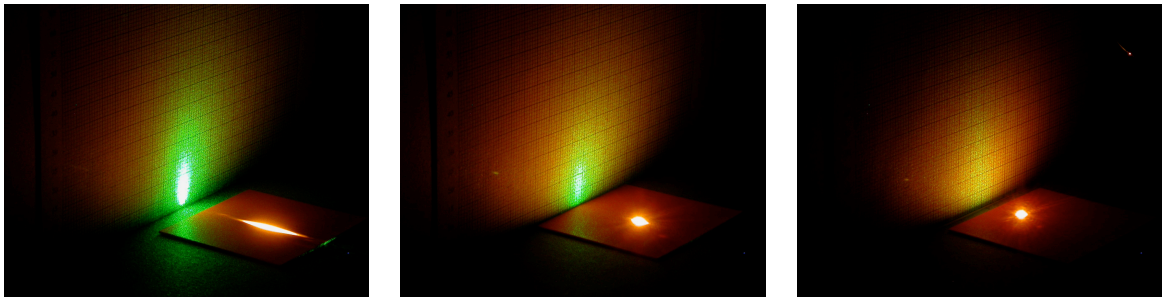

(a) (b) (c)

Figure 4.9: Reflection Patterns on a real diffuse day-glo orange cardboard sample: **a)** incident angle of less than 5 degrees; **b)** incident angle of about 20 degrees; **c)** incident angle of about 60 degrees. Note that while the bright dot where the laser hits the surface – and also parts of the reflection pattern – are a bright orange caused by the frequency shift typical for this kind of fluorescent colorant, other parts of the reflection – essentially the specular component – are still the native green of the incident laser beam. **a)** is a nice visualisation of the well-known effect that even seemingly very diffuse surfaces get more specular at grazing angles. In case **c)**, almost no green specular component is evident; practically the entire reflection is orange and has been modified by the fluorescence effects in the colorant molecules.

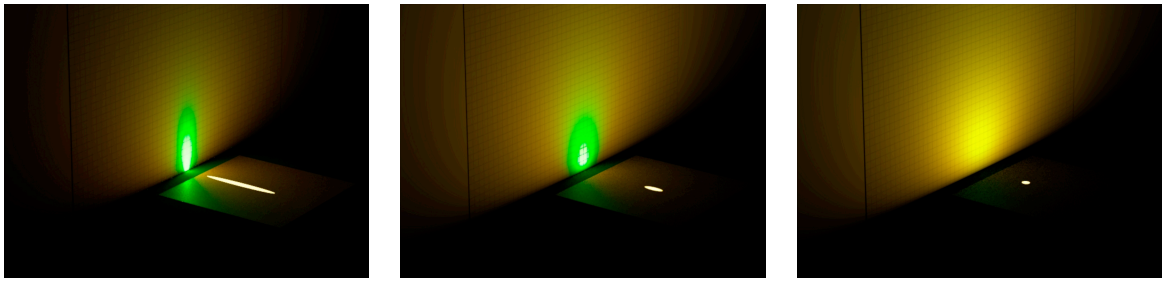

(a) (b) (c)

Figure 4.10: A rendering of a scene similar to the setting of real scene shown in figure 4.9 with similar incident angles of the laser beam: **a)** angle of incidence of 5 degrees; **b)** angle of incidence of 20 degrees; **c)** angle of incidence of 60 degrees. As described in the text, a layered surface model was used for the surface from which the laser beam is being reflected. The parameter m of the microfacet distribution was set to a value which corresponds to a mean slope angle of 17 degrees. Note that some of the visual differences to the images in figure 4.9 are due to the differences between the tone reproduction process used for the synthetic images, and the characteristics of the digital camera.

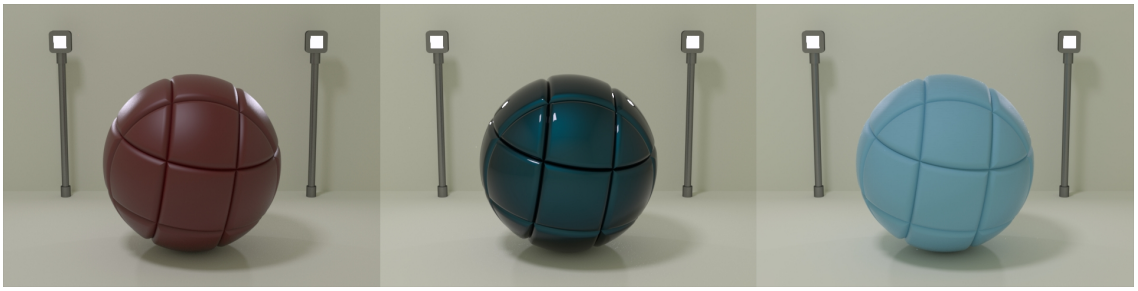

(a) (b) (c)

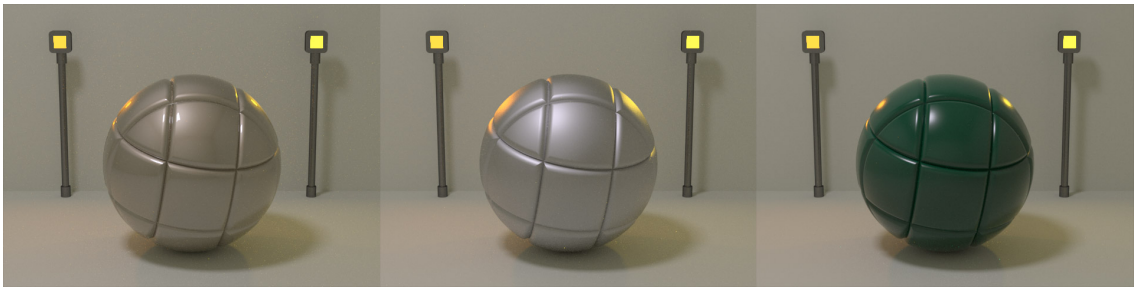

(d) (e) (f)

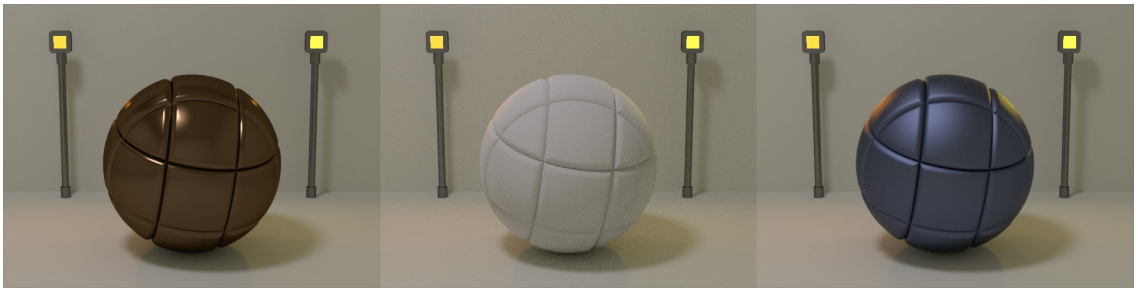

(g) (h) (i)

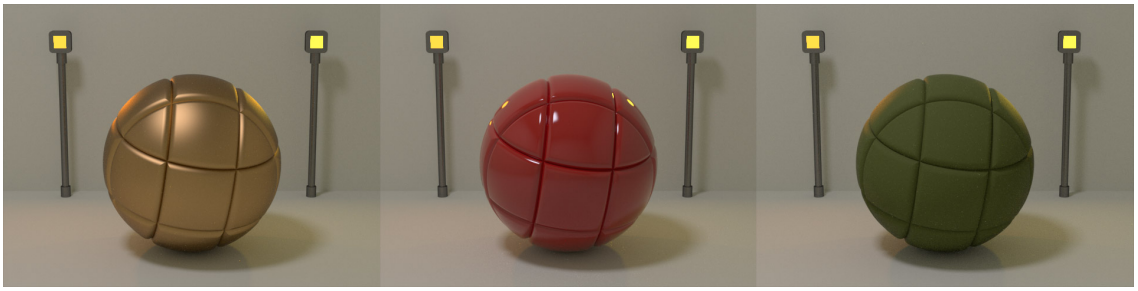

(j) (k) (l)

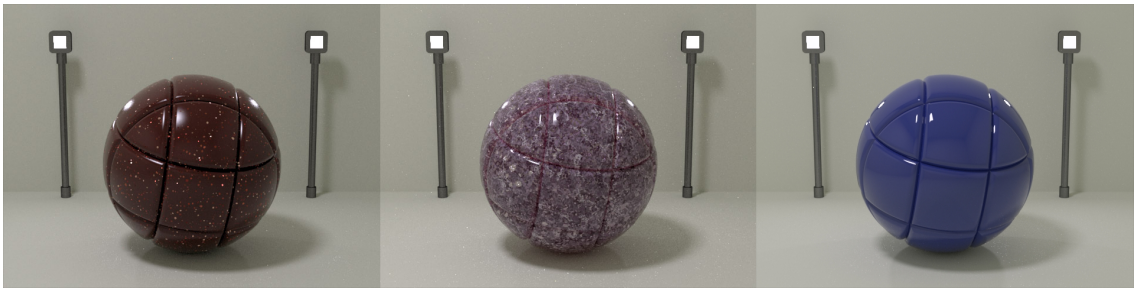

(m) (n) (o)

Figure 4.11: These surface examples were inspired by BRDF measurements from Cornell [1] and MERL [2].

Appendix A

RenderMan Shader

```
color complexFresnelReflector(
          vector I;
          normal N;
          color eta_i;
          color eta_r;
          color kappa;
        )
{

    color cos_theta = N.I;
    color etar_div_etai = eta_r / eta_i;
    color etar_div_etai_mul_k = etar_div_etai * kappa;

    color tmp = cos_theta - etar_div_etai;
    color tmp2 = cos_theta + etar_div_etai;

    color filter_parallel =  ( ( tmp * tmp ) + etar_div_etai_mul_k )
                             / ( ( tmp2 * tmp2 ) + etar_div_etai_mul_k );

    etar_div_etai_mul_k = etar_div_etai_mul_k * cos_theta;
    etar_div_etai_mul_k = etar_div_etai_mul_k * etar_div_etai_mul_k;

    tmp = 1 - etar_div_etai * cos_theta;
    tmp2 = 1 + etar_div_etai * cos_theta;

    color filter_senkrecht = ( ( tmp * tmp ) + etar_div_etai_mul_k ) /
                             ( ( tmp2 * tmp2 ) + etar_div_etai_mul_k );

    return ( filter_senkrecht + filter_parallel ) * 0.5;
}

// Blinn distribution
float blinnD( normal Nn;
              vector H;
              float exponent; )

{
    float ndoth = Nn.H;
    float D = (exponent + 2.0 ) * 0.1591549 *
              pow( max(0.0, abs(ndoth) ), exponent );
    return D;
}

// geometric attenuation factor
float geom( normal Nn;
            vector H;
            vector L;
            vector V )

{
    // Sanity check
    if ( Nn.L <= 0.0 || Nn.H <= 0.0 || V.H <= 0.0 || Nn.V <= 0.0 )
        return 0;

    float ndoth = Nn.H;
```

```
    float ndotv = Nn.V;
    float ndotl = Nn.L;
    float vdoth = V.H;

    float masking = 2 * ndoth * ndotv/vdoth;
    float shadowing = 2 * ndoth * ndotl/vdoth;
    return min( 1, min(masking, shadowing) );
}

// Based on Larry Gritz's Oren-Nayar Shader
// Note that the illuminance statement is in the main shader

color orenNayarReflector(
          normal N; vector I; vector L;
          float sigma;
          point P;
          color Cs;
        )
{
    vector Nf, IN, Eye, LN;
    color lightC = 0;
    color L1, L2;
    float C1, C2, C3;
    float theta_r, theta_i, cos_theta_i;
    float alpha, beta, sigma2, cos_phi_diff;

    Nf = faceforward (normalize(N),I);
    IN = normalize (I);
    Eye = -IN;
    theta_r = acos (Eye . Nf);
    sigma2 = sigma*sigma;

    LN = normalize(L);
    cos_theta_i = LN . Nf;
    cos_phi_diff = normalize(Eye-Nf*(Eye.Nf)).normalize(LN - Nf*(LN.Nf));
    theta_i = acos (cos_theta_i);
    alpha = max (theta_i, theta_r);
    beta = min (theta_i, theta_r);
    C1 = 1 - 0.5 * sigma2/(sigma2+0.33);

    C2 = 0.45 * sigma2 / (sigma2 + 0.09);
    if (cos_phi_diff >= 0) C2 *= sin(alpha);
    else C2 *= (sin(alpha) - pow(2*beta/PI,3));

    C3 = 0.125 * sigma2 / (sigma2+0.09) * pow ((4*alpha*beta)/(PI*PI),2);
    L1 = Cs * (cos_theta_i * (C1 + cos_phi_diff * C2 * tan(beta) +
                                (1 - abs(cos_phi_diff)) * C3 * tan((alpha+beta)/2)));
    L2 = (Cs * Cs) * (0.17 * cos_theta_i * sigma2/(sigma2+0.13) *
                        (1 - cos_phi_diff*(4*beta*beta)/(PI*PI)));
    lightC += (L1 + L2);


    return lightC;
}

color torranceSparrowReflector(
                normal Nf; vector V; vector Ln; vector H;
                color eta_i, eta_r, kappa; float m;)
{
    extern vector I;

    color cook = 0, idotn;
    float vdotn = V.Nf;
    float ldotn = Ln.Nf;

    // Sanity check
    if ( vdotn < 0.0 )
        return 0;

    float D = blinnD(Nf, H, m);
    float G = geom(Nf, H, Ln, V);
    color F;

    F = complexFresnelReflector(V, H, eta_i, eta_r, kappa);

    cook += D*G*F;

    cook /= ( 4.0 * vdotn);
```

```
    return cook;
}

// Absorption term (equation 3)
color absorption(
                normal N; vector V; vector Ln;
                color alpha;
                float d;
                )
{
    extern vector I;
    normal Nf, Nn;
    float idotn;
    color a = 1;

    Nn = normalize(N);
    Nf = faceforward(Nn, I);

    float r = 0, b = 0, g = 0;

    float ldotn = Ln.Nf;
    float vdotn = V.Nf;

    // Since we divide by the respective angles, we should take care
    // that they are not zero

    vdotn = clamp(vdotn, 0.001, 1.0);
    ldotn = clamp(ldotn, 0.001, 1.0);

    // We calculate the absorption for each colour channel
    // This is actually Beer's law

    r = exp( -alpha[0] * d * (1.0 / vdotn + 1.0 / ldotn) );
    g = exp( -alpha[1] * d * (1.0 / vdotn + 1.0 / ldotn) );
    b = exp( -alpha[2] * d * (1.0 / vdotn + 1.0 / ldotn) );

    a = (r,g,b);

    return a;
}

// Total internal reflection term (equation 4)
float tir(
                normal N; vector V; vector Ln; vector H;
                float eta;
                )
{
    extern vector I;
    extern point P;
    normal Nf, Nn;

    Nn = normalize(N);
    Nf = faceforward(Nn, I);

    float G = geom(Nf, H, Ln, V);

    float F, Kt;
    fresnel(V, H, eta, F, Kt);

    return (1-G) + (1-F) * G;
}

surface layeredMaterial (
    float sigma = 0.0;
    color eta_i = (1.5, 1.5, 1.5);              //Index of refraction top layer
    color eta_r = (1.0, 1.0, 1.0);              //Real index of refraction base layer
    color kappa = (0.0, 0.0, 0.0);              //Imaginary IOR base layer
    float m = 1;                                //Roughness top layer in degree
    float m_base = 10;                          //Roughness base layer in degree
    float samples = 32;                         //Number of EM and AO samples
    string mapname = "uffizi_cube.tif";         //Environment map name
    float reflectionType = 0;                   //1 = metallic, otherwise diffuse
    color basecolor = color (0.337,0.521,0.933);//Colour of non-metallic base material
    color alpha = color (0.337,0.521,0.933);    //Absorption index; colour is inverse
    float d = 0.5;                              //Thickness of layer
)
{
    // Convert degrees
    float beta = -log( 2.0 ) / log( cos( max(0.0001, m * 0.017453292) ) );
```

```
// Roughness for second layer
float beta_base = -log( 2.0 ) /
    log( cos( max(0.0001, ( m_base + m ) * 0.017453292) ) );

vector Nr;
Nr = faceforward(normalize(N), -I);
normal Nf = faceforward( normalize(N), I );
vector V = -normalize( I );
float fr, ft;
float depth, s;
float eta_i_avg = ( eta_i[0] + eta_i[1] + eta_i[2] ) / 3.0;
color env = 0, env_base = 0;
vector R;

color envColor = 0;
color specColor = 0;
color diff = 0, amb = 1;
color spec_base = 0;
color baseEnvColor = 0;

rayinfo("depth", depth);
s = (depth == 0) ? samples: 1;

// Ambient occlusion
float occ = 0;

gather("illuminance", P, Nf, PI/2, samples, "distribution", "cosine")
{
     occ += 1;
}

float ave = occ / samples;

// Ambient light
amb *= ambient() * ( 1 - ave / 2);

// Environment Map
if( mapname != "" )
{
    R = reflect(-V, Nr);
    R = vtransform("world", R);

    // Environment Map for top surface
    // We blur the environment map if the surface is rough

    fresnel(V, Nf, 1.0 / eta_i_avg, fr, ft);

    env = environment(
        mapname, R, "samples", samples, "blur", m/100) * fr;

    // If the second surface is metallic, it should reflect the environment as well
    if ( reflectionType == 1 )
        env_base = complexFresnelReflector(-V, Nr, eta_i, eta_r, kappa ) *
        environment( mapname, R, "samples", samples, "blur", ( m_base + m) / 100);
}

// We multiply the EM with the AO to get the selfshadowing effects
envColor = (env  * ( 1 - ave) );
env_base = ( env_base  * ( 1 - ave) );

// This is the main shader; note that only two layers are implemented (equation 2)
illuminance( P )
{

    // Top surface
    vector Ln = normalize(L);
    vector H = normalize(Ln + V);

    if ( H.V > 0.0 && H.Ln > 0.0 )
    {
        // Since the first layer is always dielectric and the parent material is
        // always air (or vacuum), we have a kappa of 0 and the IOR of the parent
        // material is 1

        if (N.Ln > 0.0)
            specColor += Cl *
                torranceSparrowReflector(Nf, V, Ln, H, 1.0, eta_i, 0.0, beta);
```

```
            // Here we compute the new directions
            vector refractLn = refract(Ln, -H, 1.0 / eta_i_avg);
            vector refractV = refract(-V, -H, 1.0 / eta_i_avg);

            refractLn  = normalize(refractLn);
            refractV  = normalize(refractV);

            // Absorption and TIR
            color a = absorption(Nf, refractV, refractLn, alpha, d);
            float t = tir(Nf, refractV, refractLn, H, eta_i_avg);

            // Environment Map for top surface
            fresnel(V, Nf, 1.0 / eta_i_avg, fr, ft);

            // Base layer
            if ( reflectionType == 1 )
            {
                // Second layer is metallic

                if (N.Ln > 0.0)
                    spec_base = Cl * torranceSparrowReflector(Nf, V, Ln, H, eta_i,
                                        eta_r, kappa, beta_base);

                baseEnvColor += env_base * ft * a * t;
                diff += spec_base * ft * a * t;

            }
            else
            {
                diff += Cl * orenNayarReflector( Nf, I, L, sigma, P, Cs ) *
                    basecolor * ft * a * t;
            }
        }
    }

    // Opacity * ( base + top + environment map + ambient illumination )
    Oi = Os;
    Ci = Cs * Oi * ( diff + baseEnvColor + envColor + specColor + amb );
}
```

Bibliography

[1] Cornell BRDF measurement database. `http://www.graphics.cornell.edu/online/\newlinemeasurements/reflectance/`.

[2] MERL BRDF measurement database. `http://www.merl.com/brdf/`.

[3] R. L. Cook and Kenneth E. Torrance. A reflectance model for computer graphics. *ACM Trans. Graph.*, 1(1):7–24, 1982.

[4] Qiang Dai, Jiaping Wang, Yiming Liu, John Snyder, Enhua Wu, and Baining Guo. The dual-microfacet model for capturing thin transparent slabs. *Comput. Graph. Forum*, 28(7):1917–1925, 2009.

[5] Craig Donner, Tim Weyrich, Eugene d'Eon, Ravi Ramamoorthi, and Szymon Rusinkiewicz. A layered, heterogeneous reflectance model for acquiring and rendering human skin. *ACM Trans. Graph.*, 27(5):1–12, 2008.

[6] Julie Dorsey and Pat Hanrahan. Modeling and rendering of metallic patinas. In *SIGGRAPH*, pages 387–396, 1996.

[7] Sergey Ershov, Konstantin Kolchin, and Karol Myszkowski. Rendering pearlescent appearance based on paint-composition modelling. *Comput. Graph. Forum*, 20(3), 2001.

[8] Sergey Ershov, Roman Ďurikovič, Konstantin Kolchin, and Karol Myszkowski. Reverse engineering approach to appearance-based design of metallic and pearlescent paints. *The Visual Computer*, 20(8-9):586–600, 2004.

[9] Xavier Granier and Wolfgang Heidrich. A simple layered rgb brdf model. *Graphical Models*, 65(4):171–184, 2003.

[10] Chet S. Haase and Gary W. Meyer. Modeling Pigmented Materials for Realistic Image Synthesis. *ACM Transactions on Graphics*, 11(4), 1992.

[11] Pat Hanrahan and Wolfgang Krueger. Reflection from layered surfaces due to subsurface scattering. *Computer Graphics*, 27(Annual Conference Series):165–174, 1993.

[12] Hideki Hirayama, Kazufumi Kaneda, Hideo Yamashita, and Yoshimi Monden. An accurate illumination model for objects coated with multilayer films. *Computers & Graphics*, 25(3):391–400, 2001.

[13] Hideki Hirayama, Kazufumi Kaneda, Hideo Yamashita, Yoshiki Yamaji, and Yoshimi Monden. Visualization of optical phenomena caused by multilayer films based on wave optics. *The Visual Computer*, 17(2):106–120, 2001.

[14] Hideki Hirayama, Yoshiki Yamaji, Kazufumi Kaneda, Hideo Yamashita, and Yoshimi Monden. Rendering iridescent colors appearing on natural objects. In *Pacific Conference on Computer Graphics and Applications*, pages 15–22, 2000.

[15] Isabelle Icart and Didier Arquès. An illumination model for a system of isotropic substrate - isotropic thin film with identical rough boundaries. In *Rendering Techniques*, pages 261–272, 1999.

[16] Isabelle Icart and Didier Arquès. A physically-based brdf model for multilayer systems with uncorrelated rough boundaries. In *Rendering Techniques*, pages 353–364, 2000.

[17] Csaba Kelemen and Laszlo Szirmay-Kalos. A microfacet based coupled specular-matte brdf model with importance sampling. In *Eurographics Short Presentations*, pages 25–34, 2001.

[18] P. Kubelka and F. Munk. Ein Beitrag zur Optik der Farbanstriche. *Z. tech. Physik*, 12:593–601, 1931.

[19] László Neumann and Attila Neumann. Photosimulation: Interreflection with arbitrary reflectance models and illuminations. *Comput. Graph. Forum*, 8(1):21–34, 1989.

[20] Addy Ngan, Frédo Durand, and Wojciech Matusik. Experimental analysis of brdf models. In *Proceedings of the Eurographics Symposium on Rendering*, pages 117–226. Eurographics Association, 2005.

[21] Michael Oren and Shree K. Nayar. Generalization of lambert's reflectance model. In *SIGGRAPH*, pages 239–246, 1994.

[22] Kenneth E. Torrance and Ephraim M. Sparrow. Theory for off-specular reflection from roughened surfaces. *J.Opt.Soc.Am*, 57(9):1105–1114, 1967.

[23] Roman Ďurikovič. Explicit method of sparkling effect simulation. *Journal of Three Dimensional Images*, 16(4):96–100, Jan 2002.

[24] Roman Ďurikovič and Tomas Ágošton. Prediction of optical properties of paints. *Central European Journal of Physics*, 5:416–427, September 2007.

[25] Gregory J. Ward. Measuring and modeling anisotropic reflection. In *SIGGRAPH*, pages 265–272, 1992.

[26] Andrea Weidlich and Alexander Wilkie. Arbitrarily layered micro-facet surfaces. In *GRAPHITE '07: Proceedings of the 5th international conference on Computer graphics and interactive techniques in Australia and Southeast Asia*, pages 171–178, 2007.

[27] Andrea Weidlich and Alexander Wilkie. Modeling aventurescent gems with procedural textures. In *Proceedings of the Spring Conference on Computer Graphics (SCCG)*, pages 1–8. ACM, April 2008.

[28] Andrea Weidlich and Alexander Wilkie. Rendering the effect of abradorescence. In *Proceedings of Graphics Interface*. ACM, March 2009.

[29] Alexander Wilkie, Andrea Weidlich, Caroline Larboulette, and Werner Purgathofer. A reflectance model for diffuse fluorescent surfaces. In Y. T. Lee, Siti Mariyam Hj. Shamsuddin, Diego Gutierrez, and Norhaida Mohd Suaib, editors, *Proceedings of the 4th International Conference on Computer Graphics and Interactive Techniques in Australasia and Southeast Asia 2006, Kuala Lumpur, Malaysia, November 29 - December 2, 2006*, pages 321–331. ACM, 2006.